
Escaping Stochastic Traps with Aleatoric Mapping Agents

Augustine N. Mavor-Parker^{1,*}Kimberly A. Young^{2,3}Caswell Barry^{2,†}Lewis D. Griffin^{4,†}

Abstract

Exploration in environments with sparse rewards is difficult for artificial agents. Curiosity driven learning — using feed-forward prediction errors as intrinsic rewards — has achieved some success in these scenarios, but fails when faced with action-dependent noise sources. We present aleatoric mapping agents (AMAs), a neuroscience inspired solution modeled on the cholinergic system of the mammalian brain. AMAs aim to explicitly ascertain which dynamics of the environment are unpredictable, regardless of whether those dynamics are induced by the actions of the agent. This is achieved by generating separate forward predictions for the mean and variance of future states and reducing intrinsic rewards for those transitions with high aleatoric variance. We show AMAs are able to effectively circumvent action-dependent stochastic traps that immobilise conventional curiosity driven agents. The code for all experiments presented in this paper is [open-sourced](#).

1 Introduction

Efficient exploration is a central problem in reinforcement learning, with particular pertinence in environments with sparse rewards — requiring agents to navigate with limited guidance (e.g. [1–3], see [4] for a review). A notable exploration method that effectively deals with sparse reward environments is curiosity driven learning; where agents are equipped with a self-supervised forward prediction model that employs prediction errors as intrinsic rewards [2, 5]. Curiosity is built upon the intuition that in unexplored regions of the environment, the forward prediction error of the agent’s internal model will be large [2]. As a result, agents are rewarded for visiting regions of the state space that they have not previously occupied. However, if a particular state transition is impossible to predict, it will trap a curious agent [3, 5]. This is referred to as the noisy TV problem (e.g. [3]), the etymology being that a naively curious agent could dwell on the unpredictability of a noisy TV screen.

There are a range of curiosity-like methods [3, 2, 6] that are designed to overcome noisy TVs (or in the terminology introduced by Shyam, Jaskowski and Gomez: “stochastic traps” [7]). However, using prediction errors as intrinsic rewards is still an open problem as current methods fail when stochastic traps are action-dependent, or require a distribution of forward prediction models [2, 6–8]. In this work we develop aleatoric mapping agents (AMAs). AMAs are intrinsic reward modules based on the work of Kendall and Gal [9], which are capable of avoiding action-dependent stochastic traps within a single prediction network. The success of our AMA approach and its connection to

*Send correspondence to: a.mavor-parker@cs.ucl.ac.uk

¹ Artificial Intelligence Centre, University College London, UK, ² Department of Cell and Developmental Biology, University College London, UK, ³ Boston University, Center for Systems Neuroscience, Graduate Program for Neuroscience, USA, ⁴ Department of Computer Science, University College London, UK

† Joint senior authors.

the work of Yu and Dayan suggests a possible role of acetylcholine in the cortex and hippocampus during exploration [10]. Namely, we hypothesise that acetylcholine could plausibly indicate expected *aleatoric* uncertainties [11] within a curiosity driven learning framework.

2 Background

2.1 Curiosity Driven Reinforcement Learning

Authors often remark that using future state prediction errors as rewards in reinforcement learning — as well as the realisation that this could lead to undesirable behaviours in stochastic environments — predates the contemporary success of Pathak’s Curiosity Driven Learning (e.g. [3, 2, 7]). Most notably, Schmidhuber [5] as well as Kaplan and Oudeyer [12] developed an intrinsic reward framework where agents are rewarded for high initial prediction errors but only if those prediction errors decrease over time.

The seminal work of Pathak et al. (2017) [2] renewed interest in curiosity for deep reinforcement learning. As a result, novel varieties of curiosity driven learning have been developed that are capable of working in stochastic environments. Burda et al. trained a curiosity-like intrinsic reward module to predict a vector output of a randomly initialised convolutional neural network (CNN) for every observation seen during exploration [3]. Exploration naturally arises as it is harder to predict the output of the random network in regions of the environment that have not been visited [3]. Further, as the output vector comes from a CNN, the method generalises to high dimensional state spaces [3].

Subsequent work by Pathak, Gandhi and Gupta addressed curiosity driven exploration using an ensemble of networks to make forward predictions. Monitoring the divergence of the networks’ predictions provided a means to avoid noisy TVs but necessitated increased computational and memory complexity [6]. Similarly, count based methods are known to reliably deal with the noisy TV problem as they do not receive intrinsic rewards for prediction errors [13]. Count based methods tabulate which states agents have occupied and reward agents for visiting states with low counts [14, 15]. They can be combined with curiosity-like methods, as performed by Raileanu and Rocktäschel [13], to avoid noisy TVs while still utilising dynamics based prediction errors when they are useful.

2.2 Exploration and Uncertainty

The uncertainty of a predictive model can be described as the sum of two *theoretically* distinct types of uncertainty: epistemic uncertainty and aleatoric uncertainty [16]. Epistemic uncertainty measures the unreliability of a model’s prediction that can be minimised with additional experience [16]. As a result, using epistemic uncertainties as intrinsic rewards means an agent will seek out dynamics it has not previously encountered (e.g. [17]).

On the other hand, prediction errors due to aleatoric uncertainties are unavoidable. They are, by definition, a result of unpredictable dynamics [16]. Prediction errors due to unpredictable dynamics immobilise curiosity driven agents as exemplified by the noisy TV problem [8].

Although theoretically attractive from an exploration point of view, quantifying epistemic uncertainty in deep forward prediction models is difficult and computationally expensive [18]. As a result, we aim to tractably approximate epistemic uncertainties by removing the aleatoric component from the total forward prediction error. This is similar to methods that separate epistemic and aleatoric uncertainties, allowing for the construction of policies that are rewarded for exploring their environments and punished for experiencing aleatoric risk [19, 20]. However, as far as we are aware we are the first to compute aleatoric uncertainties within a curiosity driven learning framework and reduce intrinsic rewards for those state transitions with high variance.

2.3 Acetylcholine

In the mammalian brain acetylcholine is a neurotransmitter implicated in a wide range of processes including learning and memory, fear, novelty detection, and attention [21–28]. Traditional views — supported by the rapid increase in acetylcholine in response to environmental novelty and demonstrable effects on neural plasticity — emphasised the role of acetylcholine as a learning signal, generating physiological changes that favour encoding of new information over retrieval [26]. We focus in particular on the role of acetylcholine during exploration in uncertain environments [25, 29, 27].

Dayan and Yu propose that in the cortex acetylcholine “signals” the expected uncertainty of top-down predictions, while cortical norepinephrine increases in correlation with experiences containing unexpected uncertainties [11]. This is supported by experimental evidence that shows acetylcholine inhibits feedback connections and strengthens sensory inputs [26], leaving an animal’s perception to be more heavily influenced by observations rather than its predictions. However, Yu and Dayan’s model does not separate epistemic and aleatoric uncertainties [25]. While the utility of quantifying epistemic uncertainties for exploration has been widely recognised in the RL literature (e.g. [17, 6]), this work demonstrates a potential use of aleatoric uncertainties for exploring agents (biological and artificial). Namely, that aleatoric uncertainties can be used to divert attention away from unpredictable dynamics when using prediction errors as intrinsic rewards. As a result, we echo the sentiment of Yu and Dayan [25], that future experimental work should aim to pinpoint what type of uncertainty (epistemic or aleatoric) acetylcholine indicates.

What’s more, we note that given acetylcholine could rise with expected aleatoric uncertainties, a reasonable hypothesis is that norepinephrine levels increase when animals are faced with epistemic uncertainties (expected and unexpected). This is related to the model proposed by Parr and Friston, which suggests that acetylcholine indicates expected uncertainties in predicted observations generated from hidden states, while norepinephrine is responsible for indicating epistemic unexpected uncertainties in hidden state transitions [30].

3 Method

3.1 Estimating Heteroscedastic Aleatoric Uncertainties

To compute heteroscedastic aleatoric uncertainty we follow Kendall and Gal, who offer an objective for regressing both the mean and expected variance in a deterministic deep learning model [9]. The method assumes a supervised learning setting, with a dataset of N inputs $\mathbf{X} = (\mathbf{x}_1, \mathbf{x}_2, \dots, \mathbf{x}_N)$ and N labels $\mathbf{Y} = (\mathbf{y}_1, \mathbf{y}_2, \dots, \mathbf{y}_N)$ [9]. The labels are defined as Gaussian distributed, with their predicted variances being a function of the inputs to the model (i.e. they are heteroscedastic) [9]. Using *maximum a posteriori* (MAP) inference with a zero-mean Gaussian prior on the network parameters θ , a proportionality expression for the posterior can be defined [9, 31].

$$p(\theta, \phi | \mathbf{X}, \mathbf{Y}) \propto \prod_{i=1}^N \mathcal{N}(\mathbf{y}_i; \mathbf{f}_\theta(\mathbf{x}_i), \mathbf{g}_\phi(\mathbf{x}_i)) \mathcal{N}(\theta, \phi; 0, \alpha^{-1} \mathbf{I}) \quad (1)$$

Where \mathbf{f}_θ are \mathbf{g}_ϕ are the neural networks used for forward prediction, θ are the network parameters for the mean prediction, ϕ are the parameters used for the variance prediction and α is a constant. Based on Kendall and Gal’s implementation, the two mean and variance prediction heads share feature extracting parameters [9]. The objective function of the model $\mathcal{L}(\theta, \phi)$, aims to maximise the negative of the right hand side of Equation 1 with respect to the model parameters [9].

$$\mathcal{L}(\theta, \phi) = \frac{1}{N} \sum_{i=1}^N \frac{1}{2} \exp(-\log \hat{\sigma}_i^2) \|\mathbf{y}_i - \hat{\mathbf{y}}_i\|^2 + \frac{\lambda}{2} \log \hat{\sigma}_i^2 + \frac{\alpha}{2} \theta^2 \quad (2)$$

To reiterate, both the estimated log variance $\log \hat{\sigma}^2$ and the estimated mean of the labels $\hat{\mathbf{y}}_i^2$ are predicted by two separate heads of a deep neural network [9]. The first and third terms of Equation 2 are the familiar mean squared error and weight decay variables, while the second term blocks the explosion of predicted variances [9]. We follow Kendall and Gal’s prescription of estimating $\log \sigma^2$ instead of σ^2 to ensure stable optimisation [9]. Furthermore, the hyperparameter λ was added, representing a quantity analogous to an aleatoric risk budget (e.g. [19, 20, 32]) of the model.

3.2 Intrinsic Rewards

Our method operates in the arena of episodic Markov decision processes (MDPs) that consist of states $s \in \mathcal{S}$, actions $a \in \mathcal{A}$, and rewards $r \in \mathcal{R} \subset \mathbb{R}$ at each timestep t [1]. In our experiments the total reward is the sum of the intrinsic reward provided by the intrinsic reward module of the agents and extrinsic rewards provided by the environment (e.g. [2, 33]).

$$r_t = \beta r_t^i + r_t^e \quad (3)$$

Where superscript, i , indicate intrinsic rewards, superscript e indicates extrinsic rewards and β is a hyperparameter that regulates the influence of intrinsic rewards on the policy. The objective of the curiosity driven agent is to learn a stochastic policy π , parametrised by ξ , that generates an action as a function of the current state s_t , which maximises the expectation of the sum of discounted future rewards (e.g. [34]).

$$\max_{\pi_\xi} \mathbb{E}_{\pi_\xi} \left[\sum_{k=0}^T \gamma^k r_{t+k} \right] \quad (4)$$

Where T is the episode length and γ is the discount factor. The forward prediction module should reward the agent for forward prediction errors unless the prediction error is impossible to reduce due to random dynamics [3]. Relying on this intuition, we craft the following intrinsic reward function for a given (s_{t+1}, \hat{s}_{t+1}) tuple; in a similar manner to [20].

$$r_t^i = \frac{1}{D} \sum_{j=1}^D ((s_{t+1,j} - \hat{s}_{t+1,j})^2 - \hat{\sigma}_{t+1,j}^2) \quad (5)$$

Where D is the dimensionality of the state observation. Note that the forward prediction module and the policy network do not share any parameters. The reward function provided by Equation 5 is non-stationary as stochastic gradient descent of the forward prediction module is performed online. More specifically, a batch of N (s_t, s_{t+1}) tuples are provided by N parallel actors at each time step t to the forward prediction module, which performs an optimisation step according to Equation 2.

4 Experiments

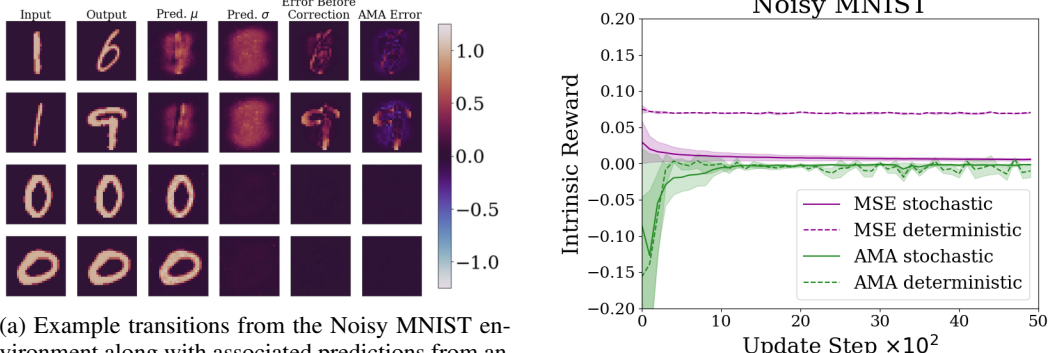
We demonstrate the performance of our method on two toy environments. The experiments isolate the problematic effects of stochastic traps on intrinsically motivated agents: both in a purely supervised setting and in the context of deep reinforcement learning.

4.1 Noisy MNIST

We begin with a supervised learning test bed, which is very similar to the noisy MNIST environment introduced by Pathak, Gandhi and Gupta [6]. The environment does not elicit any actions from an agent. Instead, the goal of the prediction network is simply to learn the mapping between N input images $\mathbf{A} = \{a_1, a_2, \dots, a_N\}$ and output images $\mathbf{B} = \{b_1, b_2, \dots, b_N\}$, where the i^{th} ($a_i \rightarrow b_i$) transition is randomly sampled from two possible transition categories. The first type of transition is completely deterministic and is cued by the input a_i having a 0 label. These transitions map onto themselves: $(a_i = 0 \rightarrow b_i = a_i = 0)$. In this case, the prediction network simply has to learn an identity mapping. The other type of transition gives 1's as input and transitions onto a random digit from 2-9: $(a_i = 1 \rightarrow b_i \in \{2, \dots, 9\})$. These transitions are the stochastic trap.

As remarked by [6], a prediction model capable of avoiding noisy TVs should learn to compute equal intrinsic rewards for both types of transitions at convergence. We train two feedforward neural networks, one standard forward prediction network (that we train with mean squared error (MSE) and will refer to as the MSE network) and one AMA network, to complete this task (adapted from an open source repository [35]). The networks are equivalent except for the fact that the AMA network has two prediction heads for the mean and variance of its prediction of the next state. Each network consists of fully connected layers (each with ReLU activations, except for the last layer, which is linear for the AMA and MSE network). The hidden layers have 784 units each except for the final hidden layer, which has 784×2 as it receives a skip connection from the input layer. In the AMA case there is only a skip connection for the mean prediction head. Both networks were optimised with Adam at a learning rate of 0.001 and a batch size of 32 [36]. Our AMA agent is optimised according to the loss function defined in Equation 2, while the MSE network uses a mean squared error (MSE) loss. The intrinsic rewards computed via these different prediction modules is presented in Figure 1.

The MSE prediction network is unable to reduce prediction errors for the stochastic transitions, leaving the stochastic transitions to produce much larger intrinsic rewards than the deterministic transitions, consistent with [6]. On the other hand, when heteroscedastic aleatoric uncertainties are



(a) Example transitions from the Noisy MNIST environment along with associated predictions from an AMA. The top two rows are examples of stochastic transitions where the prediction module of the AMA assigns high variance to the majority of the image allowing errors to be small despite the value of the output being completely unpredictable.

(b) Two reward curves for each type of network are plotted where stochastic is the $(a_i = 1 \rightarrow b_i \in \{2, \dots, 9\})$ transitions and deterministic is the $(a_i = 0 \rightarrow b_i = a_i = 0)$ transitions. Shaded area is ± 1 standard deviation. Plot inspired by [6].

Figure 1: MNIST environment visualisation and MSE and AMA performance.

estimated, the AMA prediction network is able to cut its losses by attributing high variance to the stochastic transitions, making them just as rewarding as the deterministic transitions (green line Figure 1(b)).

4.2 Deep Learning Minigrid

The Gym MiniGrid environment [37] contains a suite of highly-optimised gridworld games for computationally affordable deep reinforcement learning research. We demonstrate the efficacy our method on the MiniGrid-KeyCorridorS6R3-v0 environment and measure exploration effectiveness by the number of novel states visited during training. A $(7 \times 7 \times 3)$ observation array tracks the agent’s location and orientation as it moves around the larger grid. The channels of the observations represent semantic features (e.g. blue door, grey wall, empty, etc.) of each grid tile. The action space has seven distinct actions, expressed relative to the agent’s orientation (turn left, turn right, move forward, pickup, drop, toggle, done), one of which is selected at each timestep.

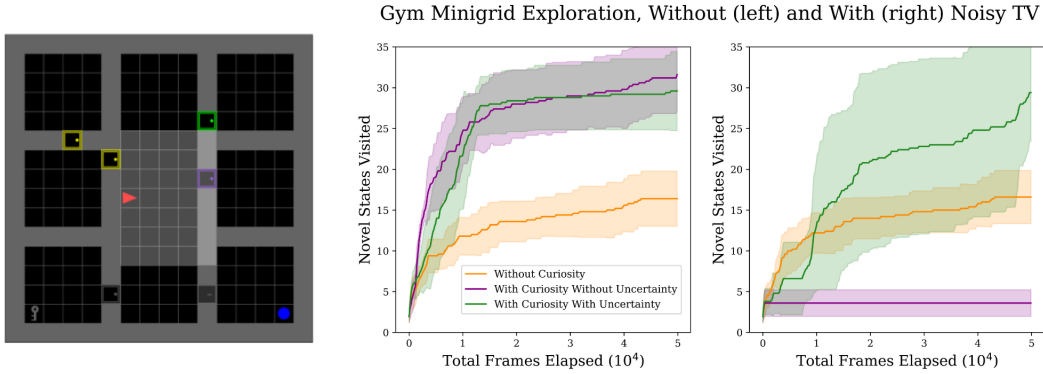
In our experimental design, a number of alterations were made to the MiniGrid environment. First, the number of frames per episode was reduced to 8. This makes efficient principled exploration more crucial, as the probability of the agent randomly discovering novel states decreases rapidly in relation to the number of frames per episode. Second, an artificial action-dependent noisy TV was added, inspired by other minigrid experiments with noisy TVs [13], consisting of a $(5 \times 5 \times 3)$ burst of random noise in the top left corner of the agent’s observation array. The values of the noise pixels were uniformly sampled across the range of possible values (representing semantic features) for the suite of minigrid environments. Whenever the agent selects the ‘done’ action the noisy TV is activated in the next observation (note that in this particular environment the ‘done’ action has no consequences for the agent, except for inducing the noisy TV). Third, all extrinsic rewards are turned off. The environment was kept constant across training episodes but different versions of the environment (with different random seeds) were used to produce the confidence regions in Figure 2.

We perform policy optimization with the synchronous actor critic (A2C) algorithm [34]. Our implementation is adapted from a starter repository recommended in the Gym MiniGrid README [38]. The actor critic architecture begins with 3 (2×2) convolutional layers with $(16, 32, 64)$ output channels for each layer and a Maxpool layer after the first convolution. A ReLU is applied to all convolutional layers. The features extracted are then fed to two MLPs representing the actor and critic heads with the two layers each having dimension of $(64, 64, 7)$ and $(64, 64, 1)$. A Tanh activation is used in the penultimate layer of both actor-critic heads. The actor critic weights were optimised with RMSProp [39] at a learning rate of 0.001. We use 16 parallel actors during training.

The forward prediction module works in the observation space as opposed to a learned feature space as is implemented in other curiosity driven methods [2, 3, 13]. Using pixel based predictions is not a limitation of our method, but was chosen due to its simplicity of implementation and the natural interpretability of predictions when debugging. The forward prediction model consists of a feature

Table 1: Frequency of the actions selected by the MSE and AMA agents across one run in the Minigrid environment

Action	Mean Frequency MSE	Mean Frequency AMA
left	76	19457
right	113	13496
forward	63	15459
pickup	54	127
drop	54	95
toggle	261	81
done (stochastic trap)	49427	1336



(a) Rendering of the MiniGrid-KeyCorridorS6R3-v0 environment. The highlighted grey rectangle represents the receptive field of the agent.

(b) Comparison of different agents averaged over 5 runs (different random seeds) with and without an action-dependent stochastic trap present. All policies are optimised with A2C. The agents differ in how their intrinsic rewards are computed: No rewards for the Baseline agent, mean squared error for the vanilla approach and our method for AMA. Shaded is area is ± 1 standard deviation.

Figure 2: Deep learning minigrid results.

extracting CNN architecture (1 layer with 32 output channels), which ingests an observation at s_t followed by two separate fully-connected network heads predicting the mean and log variance of the pixels of s_{t+1} . The two hidden layers for both heads have (621, 147) hidden units each. ReLU is applied throughout the intrinsic reward model except for in the final layer where no activation is used for the forward prediction and ReLU is used for the log variance prediction. Our architecture is based in part on other intrinsic reward models that performed well on gym-minigrid environments [13]. The intrinsic reward module was optimised with the Adam optimizer at a learning rate of 0.0001 for the AMA agent and 0.001 for the MSE agent [39].

The intrinsic rewards were scaled by a factor of 10 in both cases. All rewards were normalised with a running mean and standard deviation for the AMA agent and the MSE agent, as is recommended for intrinsic rewards (e.g. [8, 33]). All the settings described were selected by hyperparameter tuning (via grid search) the respective agents to visit as many states as possible averaged across environments with and without a noisy TV present. For a full description of the all the underlying RL hyperparameters we refer the reader to the public repository [38].

As shown in Figure 2(b) when no noisy TV is present, the MSE curiosity provides a performance boost (right panel Figure 2(b)). However, the presence of the noisy TV has a disastrous effect on the MSE curiosity agent (left panel Figure 2(b)). On the other hand, the AMA agent maintains a performance boost from its intrinsic rewards with and without the presence of an action dependent noisy TV.

5 Conclusion

We have shown AMAs are able to avoid action-dependent stochastic traps that destroy the exploration capabilities of conventional curiosity driven agents [8], both in a supervised setting and a deep RL setting. AMAs complete such a feat in a computationally tractable manner by decreasing intrinsic rewards in regions with high estimated aleatory using the predictions of a single deterministic forward prediction network.

Given the success of AMAs, we observe that there are three curiosity-like deep RL models that might accurately mimic the role of acetylcholine in exploration. The first two possibilities being equivalent to the descriptions provided by Yu and Dayan [25]. Specifically, that acetylcholine represents model “ignorance” [25] (expected epistemic uncertainty) or, alternatively, that it represents the unpredictability of the environment (expected aleatoric uncertainty) [10]. A third possibility, suggested by the Random Network Distillation model presented by Burda et al., is consistent with the cholinergic role in novelty signalling [3, 24].

We build on the foundation laid by Yu and Dayan [25], arguing that future experimental work should aim to decipher whether acetylcholine indicates expected epistemic uncertainties, expected aleatoric uncertainties or simply novelty. Then, direct comparisons can be made between the uncertainties signalled by biological and artificial agents to further research in reinforcement learning and neuroscience alike. In future work, we aim to further verify the efficacy of the AMA method in deep reinforcement learning settings, by performing experiments on popular game playing and simulated 3D environments.

Acknowledgments and Disclosure of Funding

Augustine N. Mavor-Parker is supported by the EPSRC project reference 2250955. Caswell Barry was funded by a Wellcome Senior Research Fellowship (212281/Z/18/Z). Augustine N. Mavor-Parker would like to thank Changmin Yu, Andrea Banino, Charles Blundell, Maximillian Mozes, Kimberly Mai and Felix Biggs for their comments on this project.

References

- [1] Richard S Sutton and Andrew G Barto. *Reinforcement learning: An introduction*. MIT press, 2018.
- [2] Deepak Pathak, Pulkit Agrawal, Alexei A Efros, and Trevor Darrell. Curiosity-driven exploration by self-supervised prediction. In *International Conference on Machine Learning*, pages 2778–2787. PMLR, 2017.
- [3] Yuri Burda, Harrison Edwards, Amos Storkey, and Oleg Klimov. Exploration by random network distillation. *arXiv preprint arXiv:1810.12894*, 2018.
- [4] Lilian Weng. Exploration strategies in deep reinforcement learning. *lilianweng.github.io/lil-log*, 2020.
- [5] Jürgen Schmidhuber. Adaptive confidence and adaptive curiosity. In *Institut für Informatik, Technische Universität München, Arcisstr. 21, 8000 München 2*. Citeseer, 1991.
- [6] Deepak Pathak, Dhiraj Gandhi, and Abhinav Gupta. Self-supervised exploration via disagreement. *arXiv preprint arXiv:1906.04161*, 2019.
- [7] Pranav Shyam, Wojciech Jaśkowski, and Faustino Gomez. Model-based active exploration. In *International Conference on Machine Learning*, pages 5779–5788, 2019.
- [8] Yuri Burda, Harri Edwards, Deepak Pathak, Amos Storkey, Trevor Darrell, and Alexei A Efros. Large-scale study of curiosity-driven learning. *arXiv preprint arXiv:1808.04355*, 2018.
- [9] Alex Kendall and Yarin Gal. What uncertainties do we need in bayesian deep learning for computer vision? In *Advances in neural information processing systems*, pages 5574–5584, 2017.

[10] Peter Dayan and J Yu Angela. Expected and unexpected uncertainty: Ach and ne in the neocortex. In *Advances in neural information processing systems*, pages 173–180, 2003.

[11] Peter Dayan and J Angela Yu. Ach, uncertainty, and cortical inference. In *Advances in neural information processing systems*, pages 189–196, 2002.

[12] Frederic Kaplan and Pierre-Yves Oudeyer. In search of the neural circuits of intrinsic motivation. *Frontiers in neuroscience*, 1:17, 2007.

[13] Roberta Raileanu and Tim Rocktäschel. Ride: Rewarding impact-driven exploration for procedurally-generated environments. In *International Conference on Learning Representations*, 2020.

[14] Alexander L Strehl and Michael L Littman. An analysis of model-based interval estimation for markov decision processes. *Journal of Computer and System Sciences*, 74(8):1309–1331, 2008.

[15] Marc G Bellemare, Sriram Srinivasan, Georg Ostrovski, Tom Schaul, David Saxton, and Remi Munos. Unifying count-based exploration and intrinsic motivation. *arXiv preprint arXiv:1606.01868*, 2016.

[16] Eyke Hüllermeier and Willem Waegeman. Aleatoric and epistemic uncertainty in machine learning: A tutorial introduction. *arXiv preprint arXiv:1910.09457*, 2019.

[17] Ian Osband, Charles Blundell, Alexander Pritzel, and Benjamin Van Roy. Deep exploration via bootstrapped dqn. In *Advances in neural information processing systems*, pages 4026–4034, 2016.

[18] Yarin Gal. Uncertainty in deep learning. *University of Cambridge*, 1(3), 2016.

[19] Stefan Depeweg, Jose-Miguel Hernandez-Lobato, Finale Doshi-Velez, and Steffen Udluft. Decomposition of uncertainty in bayesian deep learning for efficient and risk-sensitive learning. In *International Conference on Machine Learning*, pages 1184–1193. PMLR, 2018.

[20] William R Clements, Benoît-Marie Robaglia, Bastien Van Delft, Reda Bahi Slaoui, and Sébastien Toth. Estimating risk and uncertainty in deep reinforcement learning. *arXiv preprint arXiv:1905.09638*, 2019.

[21] Charan Ranganath and Gregor Rainer. Neural mechanisms for detecting and remembering novel events. *Nature Reviews Neuroscience*, 4(3):193–202, 2003.

[22] Giancarlo Pepeu and Maria Grazia Giovannini. Changes in acetylcholine extracellular levels during cognitive processes. *Learning & memory*, 11(1):21–27, 2004.

[23] Elio Acquas, Catriona Wilson, and Hans C Fibiger. Conditioned and unconditioned stimuli increase frontal cortical and hippocampal acetylcholine release: effects of novelty, habituation, and fear. *Journal of Neuroscience*, 16(9):3089–3096, 1996.

[24] Caswell Barry, James G Heys, and Michael E Hasselmo. Possible role of acetylcholine in regulating spatial novelty effects on theta rhythm and grid cells. *Frontiers in neural circuits*, 6:5, 2012.

[25] J Angela Yu and Peter Dayan. Uncertainty, neuromodulation, and attention. *Neuron*, 46(4):681–692, 2005.

[26] Michael E Hasselmo. The role of acetylcholine in learning and memory. *Current opinion in neurobiology*, 16(6):710–715, 2006.

[27] MG Giovannini, A Rakovska, RS Benton, M Pazzaglia, L Bianchi, and G Pepeu. Effects of novelty and habituation on acetylcholine, gaba, and glutamate release from the frontal cortex and hippocampus of freely moving rats. *Neuroscience*, 106(1):43–53, 2001.

[28] Vinay Parikh, Rouba Kozak, Vicente Martinez, and Martin Sarter. Prefrontal acetylcholine release controls cue detection on multiple timescales. *Neuron*, 56(1):141–154, 2007.

- [29] CM Thiel, JP Huston, and RKW Schwarting. Hippocampal acetylcholine and habituation learning. *Neuroscience*, 85(4):1253–1262, 1998.
- [30] Thomas Parr and Karl J Friston. Uncertainty, epistemics and active inference. *Journal of The Royal Society Interface*, 14(136):20170376, 2017.
- [31] Christopher M Bishop. *Pattern recognition and machine learning*. Springer, 2006. p.30.
- [32] Hannes Eriksson and Christos Dimitrakakis. Epistemic risk-sensitive reinforcement learning. *arXiv preprint arXiv:1906.06273*, 2019.
- [33] Adrià Puigdomènech Badia, Pablo Sprechmann, Alex Vitvitskyi, Daniel Guo, Bilal Piot, Steven Kapturowski, Olivier Tieleman, Martín Arjovsky, Alexander Pritzel, Andrew Bolt, et al. Never give up: Learning directed exploration strategies. *arXiv preprint arXiv:2002.06038*, 2020.
- [34] Volodymyr Mnih, Adria Puigdomenech Badia, Mehdi Mirza, Alex Graves, Timothy Lillicrap, Tim Harley, David Silver, and Koray Kavukcuoglu. Asynchronous methods for deep reinforcement learning. In *International conference on machine learning*, pages 1928–1937, 2016.
- [35] Xingyu Liao. pytorch simple autoencoder. https://github.com/L1aoXingyu/pytorch-beginner/blob/master/08-AutoEncoder/simple_autoencoder.py, 2020.
- [36] Diederik P Kingma and Jimmy Ba. Adam: A method for stochastic optimization. *arXiv preprint arXiv:1412.6980*, 2014.
- [37] Maxime Chevalier-Boisvert, Lucas Willems, and Suman Pal. Minimalistic gridworld environment for openai gym. <https://github.com/maximecb/gym-minigrid>, 2018.
- [38] Lucas Willems. RL Starter Files. <https://github.com/lcswillems/rl-starter-files>, 2020.
- [39] Tijmen Tieleman and Geoffrey Hinton. Rmsprop gradient optimization. URL http://www.cs.toronto.edu/tijmen/csc321/slides/lecture_slides_lec6.pdf, 2014.